# Time-resolved analysis of cavitation induced by CW lasers in absorbing liquids

**J.C. Ramirez-San-Juan,[1]* E. Rodriguez-Aboytes, [1] A. E. Martinez-Canton,[1] O. Baldovino-Pantaleon,[2] A. Robledo-Martinez,[3] N. Korneev,[1] and R. Ramos-Garcia[1]**

[1]*Departamento de Optica, Instituto Nacional de Astrofisica, Optica y Electronica, Apartado Postal 51 y 216, 72000 Puebla, Pue. Mexico*

[2]*Universidad Autónoma de Tamaulipas, Unidad Académica Multidisciplinaria Reynosa-Rhode, 88779 Reynosa, Mexico.*

[3]*Universidad Autonoma Metropolitana, Departamento de Energia, Av. San Pablo 180,02200, Mexico D.F., Mexico*

**jcram@inaoep.mx*

**Abstract:** We present novel results on thermocavitation using a CW medium-power near infrared laser (λ=975 nm) focused into a saturated copper nitrate saline solution. Due to the large absorption coefficient at the laser wavelength, the solution can be heated to its superheat limit ($T_{sh}$~270-300°C). Superheated water undergoes explosive phase transition around $T_{sh}$ producing approximately half-hemispheric bubbles (γ~0.5) in close contact with the substrate. We report the temporal dynamic of the cavitation bubble, which is much shorter than previously reported under similar conditions. It was found that the bubble radius and pressure wave amplitude emitted on bubble collapse decreases exponentially with the power laser. Thermocavitation can be a useful tool for the generation of ultrasonic waves and controlled ablation for use in high-resolution lithography.



**OCIS codes:** (190.4870) Photothermal effects; (170.1065) Acousto-optics; (280.3375) Laser induced ultrasonics; (280.5395) Plasma diagnostics.

## References and links

1. J. M. Michel, and J. P. Franc, *Fundamentals of Cavitation* Springer 2004.
2. C. E. Brennen, *Cavitation and Bubble Dynamics* Oxford University Press, USA (1995)
3. F. R. Young, *Cavitation*, Imperial College Press, London (1999).
4. L. Azar "Cavitation in Ultrasonic Cleaning and Cell Disruption" Controlled Environments February, 14–17 (2009).
5. W. Lauterborn, ed., "Cavitation and inhomogeneities in underwater acoustics" Springer-Verlag (1980).
6. R. G. Brewer, and K. E. Rieckhoff, "Stimulated Brillouin scattering in liquids," Phys. Rev. Lett. **13**(11), 334–336 (1964).
7. E. F. Carome, C. E. Moeller, and N. A. Clark, "Intense Ruby-Laser-Induced Acoustic Impulses in Liquids," J. Acoust. Soc. Am. **40**(6), 1462–1466 (1966).
8. W. Lauterborn, "High-speed photography of laser-induced breakdown in liquids," Appl. Phys. Lett. **21**(1), 27–29 (1972).
9. C. A. Sacchi, "Laser-induced electric breakdown in water," J. Opt. Soc. Am. B **8**(2), 337–345 (1991).
10. P. A. Barnes, and K. E. Rieckhoff, "Laser-induced underwater sparks," Appl. Phys. Lett. **13**(8), 282–284 (1968).
11. K.-T. Byun, H.-Y. Kwak, and S. W. Karng, "Bubble Evolution and Radiation Mechanism for Laser-Induced Collapsing Bubble in Water," Jpn. J. Appl. Phys. **43**(No. 9A), 6364–6370 (2004).
12. J. Noack, D. X. Hammer, G. D. Noojin, B. A. Rockwell, and A. Vogel, "Influence of pulse duration on mechanical effects after laser-induced breakdown in water," J. Appl. Phys. **83**(12), 7488–7495 (1998).
13. C. D. Ohl, T. Kurz, R. Geisler, O. Lindau, and W. Lauterborn, "Bubble dynamics, shock waves and sonoluminiscence," Philos. Trans. R. Soc. Lond. A **357**(1751), 269–294 (1999).
14. S. F. Rastopov, and A. T. Sukhodol'sky, "Cluster nucleation in the process of CW laser induced thermocavitation," Phys. Lett. A **149**(4), 229–232 (1990).
15. S. F. Rastopov, and A. T. Sukhodolsky, "Sound generation by thermocavitation induced CW-laser in solutions," Proc. SPIE **1440**, 127–134 (1990).
16. B. P. Barber, R. A. Hiller, R. Lijfstedt, S. J. Putterman, and K. R. Weninger, "Defining the unknowns of sonoluminescence," Phys. Rep. **281**(2), 65–143 (1997).
17. J. C. Ramirez-San-Juan, *et al*., "Cavitation induced by CW lasers in liquids," Proc. SPIE **7562–37**, 1–5 (2010).

#120889 - $15.00 USD Received 2 Dec 2009; revised 15 Jan 2010; accepted 24 Jan 2010; published 12 Apr 2010

18. V. P. Skripov, and P. A. Pavlov, "Explosive boiling of liquids and fluctuation nucleus formation," High Temp. (USSR) **8**, 782–787 (1970).
19. O. Yavas, P. Leiderer, H. K. Park, C. P. Grigoropoulos, C. C. Poon, W. P. Leung, N. Do, and A. C. Tam, "Optical reflectance and scattering studies of nucleation and growth of bubbles at a liquid-solid interface induced by pulsed laser heating," Phys. Rev. Lett. **70**(12), 1830–1833 (1993).
20. P. Kafalas, and A. P. Ferdinand, Jr., "Fog droplet vaporization and fragmentation by a 10.6-μm laser pulse," Appl. Opt. **12**(1), 29–33 (1973).
21. V. P. Skripov, *Metastable Liquids*. John Wiley and Sons, New York (1974).
22. A. Vogel, W. Lauterborn, and R. Timm, "Optical and acoustic investigations of the dynamics of laser-produced cavitation bubbles near a solid boundary," J. Fluid Mech. **206**(-1), 299–338 (1989).
23. A. Vogel, and W. Lauterborn, "Acoustic transient generation by laser-produced cavitation bubbles near a solid boundaries," J. Acoust. Soc. Am. **84**(2), 719–731 (1988).
24. Private communication from RP Acoustics,
25. A. Y. Çengel, *Heat transfer: A practical approach*, Pag. 23 McGraw-Hill, New York 2003.

## 1. Introduction

Cavitation, the formation of cavities inside liquids, is part of everyday life experience. Cavitation is created, for example, whenever a liquid is agitated violently, like in boat propellers and hydraulic machinery [1–3]. The bubbles´ collapse can damage the container or structure wherever the liquid is flowing. On the other hand, cavitation may be a useful tool in fields such as medicine, where it can be used for lithotripsy and drug delivery [4]. According to Lauterborn [5], cavitation can be classified in four types depending on the physical mechanism of creation: *i)* acoustic, *ii)* hydraulic *iii)* particle and *iv)* optic. A great deal of research has been carried out in the four areas of cavitation as reported in Ref. 1-3 and references therein. In this paper, we deal with optic cavitation exclusively. Laser-induced cavitation is generally produced by short laser pulses focused on liquids [6–9]. The light's intensity at the focus is so high that nonlinear absorption and/or avalanche ionization leads to plasma formation. Due to the high absorption coefficient of plasma in the visible, it can be rapidly heated by the laser beam to temperatures on the order of 7000-10000°K [10,11] and pressures as high as MPa or even GPa [12,13] leading to water rapid vaporization producing audible acoustic shock waves. In 1990, Rastopov et.al [14,15] reported for the first time cavitation in dye-doped binary solutions, i.e liquids with different boiling temperatures. The physical mechanism of cavitation is the creation of an overheated region (120-240 °C depending on beam power, alcohol/water concentration and absorption coefficient) at the focal point, followed by explosive liquid evaporation. Once the bubble reaches a cooler region it collapses very rapidly creating a hydraulic shock wave. This mechanism of cavitation was termed thermocavitation. Despite the fact that thermocavitation may sound attractive because its low power requirement and its many potential applications, not much attention has been given to this topic in recent times.

In this paper, we present novel results on thermocavitation in saturated copper nitrate saline solution. We report the temporal dynamic of the cavitation bubble, which turns out to be much shorter than previously reported by Rastopov [15]. It was found that the bubble's radius and amplitude of the shock wave decreases exponentially with the beam power. Thermocavitation can be a useful tool for the generation of ultrasonic waves and controlled ablation for use in high-resolution photolithography.

## 2. Experiment

A beam from a laser diode ($\lambda$=975 nm) is expanded, collimated and focused down with a 10x microscope objective (beam waist of 12 μm at focus) into a cuvette filled with a saturated solution of copper nitrate [see Fig. 1(a)]. The absorption coefficient of the solution is $\alpha$=135 $\mathbf{c}m^{-1}$, so the light is strongly absorbed near the entrance wall. The pressure of the shock waves generated by the expansion and collapse of the bubbles is measured with a calibrated hydrophone (RP Acoustic Mod. RP 11s) placed 4 mm above the bubble formation. In order to measure the temporal evolution of the bubble's radius [16] a collimated green beam ($\lambda$ = 532 nm) probes the region where the infrared beam is focused. The scattered light from the green

#120889 - $15.00 USD Received 2 Dec 2009; revised 15 Jan 2010; accepted 24 Jan 2010; published 12 Apr 2010

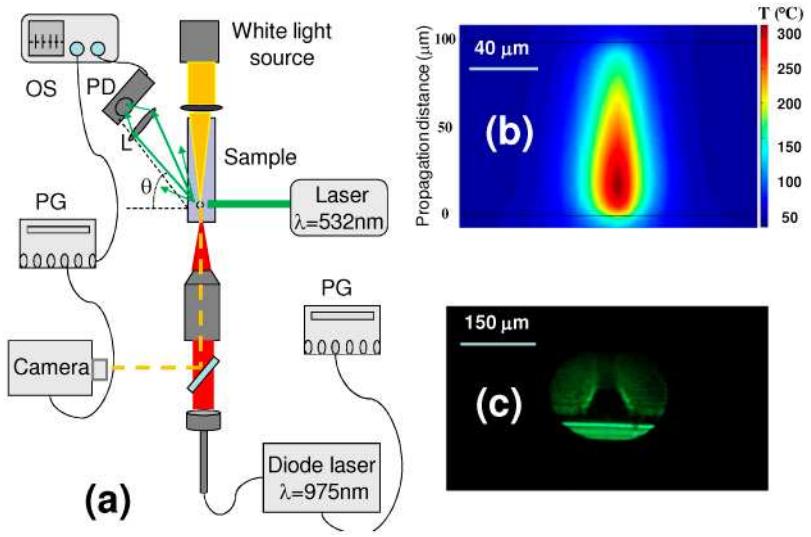


Fig. 1.( a) Experimental setup used for the generation and analysis of single bubble cavitation. PG is a pulse-delay generator, OS is digital oscilloscope and PD is a fast photodetector; (b) temperature distribution of a 119 mW focused beam inside the solution. The hottest (300°C) region is located ~20 μm above the entrance wall; (c) shadowgram of the hot region produced by a focused beam of power 119 mW just before cavitation takes place.

beam is measured at an angle θ = 60° from the forward direction using a fast photodetector (EOT Mod. ET-2030 rise time 0.3 ns). Both signals from the photodetector and hydrophone are recorded on a digital oscilloscope. The microscope objective is used to project the bubble image onto a streak camera (Hamamatsu Mod. C2830) as shown in Fig. 1(a). The camera could operate either in the frame or streak mode. Additionally, lateral coherent or incoherent illumination was used to image the bubble since top view illumination do not gives information about the asymmetry of the bubble. The light scattered by the bubble triggered a digital oscilloscope. A second pulse-delay generator unit was used to trigger the streak camera (operated in the frame mode) in order to obtain different snap shots of the bubble dynamics. Using the fast camera in the streak mode provided the bubble's instant radii as function of time.

### 3. Results

Cavitation is a repetitive process under CW illumination whose frequency depends linearly on the beam intensity [15,17]. The beam intensity is changed by displacing the cuvette around the focus to optimize the cavitation frequency to ~ 300 Hz. However, the frequency can be increased at least an order of magnitude with tighter focusing [17]. Very often it is possible to generate more than one bubble making the analysis of its dynamic hard to interpret. In order to produce a single bubble, we modulated the laser current with a single square pulse whose width was controlled by a pulse-delay generator. The power delivered by laser remains constant along the square pulse. Figure 2 shows the cavitation time $\tau_{cav}$, defined as the time at which a single cavitation occurs after the laser has been turned on. Note that the $\tau_{cav}$ decreases exponentially with power as indicated by the red line which represent an exponential decay fit.

In absorbing solutions, a tightly focused beam can induce temperature jumps well above its boiling temperature. As a result, phase explosion or explosive boiling is possible. The maximum temperature at which liquid boils explosively is called the superheat limit. Several techniques have been implemented to measure the superheat limit of water including T-jumps [18], short pulse laser [19] or high power CW $CO_2$ laser [20]. Superheat limits for water has been determined to be in the range 270-302°C [18–20]. In our experiments temperature

#120889 - $15.00 USD Received 2 Dec 2009; revised 15 Jan 2010; accepted 24 Jan 2010; published 12 Apr 2010

measurements are hard to perform because of the small dimensions of the heated volume ($\mu m^3$) and high heating rates (up to ~$10^5$ °C/sec) involved. So, we decided to perform numerical simulations in order to estimate the maximum temperature achieved in a saturated solution of copper nitrate.

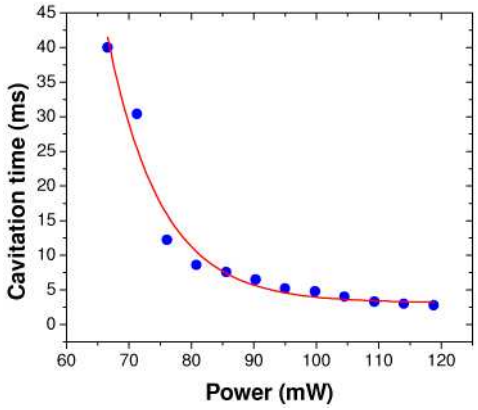


Fig. 2. Cavitation time as function of the beam power. Solid line represents a fit to an exponential decay function

We model a focused Gaussian beam which is propagated into a 100 μm thick cell (thicker cell gives basically the same results) filled with saturated solution of copper nitrate and calculate the temperature rise induced by the light absorption as function of time by solving the time dependent heat transfer equation:

$$\rho C \frac{\partial T}{\partial t} + \nabla \cdot \left(-k \nabla T\right) = Q, \tag{1}$$

where $\rho$ is the density, $C$ is the specific heat capacity, and $k$ is the thermal conductivity of the water respectively. $Q$ is the heat source term given by $Q=\alpha I$, where $\alpha$ is the absorption coefficient of the solution and $I$ is the beam's intensity with Gaussian profile. In order to solve Eq. (1) we made a crude approximation: it was assumed that the thermodynamic properties of water are not affected by the addition of copper nitrate and its effect is reflected only on the absorption coefficient of water. Figure 1(b) shows the temperature profile at the cavitation time $t_{cav}$=2.8 ms corresponding at the maximum intensity available from our laser $I_{max}$=2.5x$10^4$ W/$cm^2$ (P=119 mW and beam waist of 12 μm). Temperature values as high as ~300 °C can be achieved ~17 μm from the entrance interface. On the other hand, the temperature rise for the threshold intensity to produce a single cavitation, $I_{thr}$≈1.5x$10^4$ W/$cm^2$, reaches 270 °C in 40 ms (P=69 mW). These temperature values agree well with those reported in Refs. 18-20.

Figure 1(c) shows a fast-frame shadowgram of the hot region (dark central area) taken just before cavitation. The bottom horizontal line represents the wall-solution interface. Note the good qualitative agreement between theory predictions and experiment. The thick faint line observed above the hot region, corresponds to the laser-induced water flow. This effect was not taken into account in our simulations, so the actual temperature of the hot region may be smaller than the calculated value. Nevertheless, our simulations indicate that temperatures well above the boiling temperature can easily be achieved with focused beams in highly absorbing solutions. Once the superheat limit is reached, a violent phase explosion is observed producing an expanding vapor bubble in close proximity to the interface.

Figure 3(a) shows the bubble radius measured with the streak camera, the scatter signal taken from the photodetector, and the pressure wave generated by the collapse of the bubble for $I_{max}$. The laser is turned on for 3.5 ms, however only 200 μs are displayed because this

#120889 - $15.00 USD Received 2 Dec 2009; revised 15 Jan 2010; accepted 24 Jan 2010; published 12 Apr 2010

interval contains the relevant information. For t<2.8 ms, the beam is just heating the solution up; when the temperature approaches the superheat limit (at ~2.8 ms), the probability of explosive phase transition increases exponentially [21] and eventually the superheated water around the hottest region is explosively vaporized. The high pressure of the fully evaporated water moves outwards against the surrounding liquid producing a pressure wave of very low amplitude [2.3 KPa, not visible on the scale shown in Fig. 3(a)]. This is in contrast to short-pulse induced cavitation, where vaporization of water by the hot plasma produce pressure waves as high as 3 GPa [11,12]. Once the bubble is created, it scatters the green light and therefore the signal on the photodetector increases rapidly reaching its maximum in 43 μs and then slowly decreases to zero in approximately ~ 1 ms.

The square root of the photodetector signal ($PD^{1/2}_{signal}$) is proportional to the bubble's radius [16]. However, as it will be shown later, this is true only during the first 40-60 μs. This time scale corresponds to the time the bubble's radius reaches its maximum. In order to correctly measure the bubble diameter, a streak camera was employed. The bubble's radius reaches its maximum ($r_{max}$~200 μm) in 43 μs and then collapses rapidly in just 20 μs, i.e. the conversion of potential energy to kinetic energy is faster that the corresponding conversion from kinetic to potential expansion stage. In the same figure, it can be observed that the measured bubble radius coincide very well with $PD^{1/2}_{signal}$ during the expansion bubble stage. In previous studies, the bubble's lifetime was estimated from the scattered signal leading to an overestimation of the bubble's lifetime [15]. We believe that this slow decay of the scattered signal comes from the strong refraction near the surface wall due to the hot region produced by the laser beam.

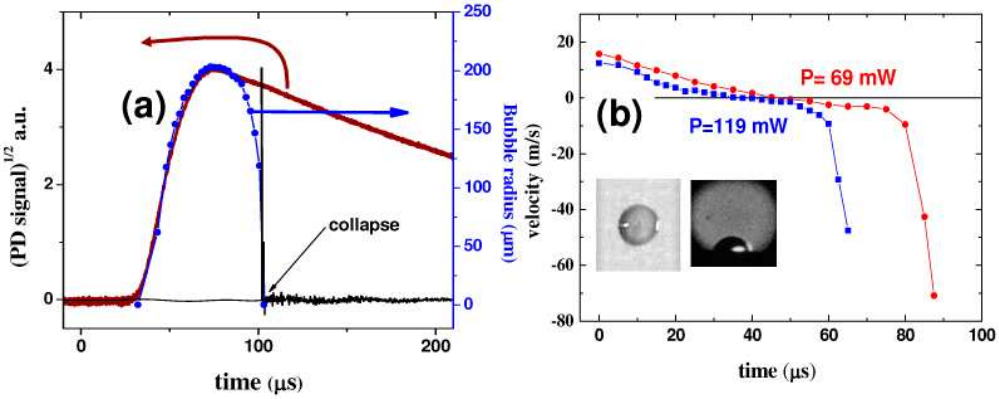


Fig. 3. (a) Representative traces of the square root of the light scattered by the bubble (thick magenta line), bubble's radius (blue circles) obtained from the streak camera and pressure wave generated at the collapse of the bubble (indicated by the black arrow) for $P_{max}$=119 mW. Note that the bubble radius measured by the streak camera matches the square root of the scattered signal only during expansion. (b) Velocity of the bubble wall for $P_{thr}$=69 and $P_{max}$=119 mW. The inset shows a typical snap shot of the bubble near its maximum radius for top view (left) and side view (right).

The inset of Fig. 3(b) shows a typical fast-frame of the bubble near its maximum radius from side view (left) and top view (right) using incoherent light illumination. Note that the bubble is attached to the substrate and therefore approximately only one half bubble is produced i.e. γ~0.5 ($\gamma=h/R_{max}$ where $h$ is the distance from the wall to the center of the bubble and $R_{max}$ is the maximum bubble radius). It is worth to mention that the bubble is always attached to the substrate for all powers at all times. By changing the concentration of salt in water or using a laser with emission in the visible it is possible to obtain γ >>1and thus obtain spherical bubbles. However, it was not possible to do it due to the limited power of our laser even if we used a 100x microscope objective to reduce the spot size. Nevertheless it should be of great interest to study the cavitation of spherical bubbles away from the substrate.

#120889 - $15.00 USD Received 2 Dec 2009; revised 15 Jan 2010; accepted 24 Jan 2010; published 12 Apr 2010

Figure 3(b) also shows the velocity of the bubble walls for two powers: 69 mW and 119 mW, which corresponds to the threshold power for cavitation and our laser's maximum power, respectively. It can be observed that the velocity of the bubble walls slowly decreases from its initial value (~17 m/s) as the bubble expands. It stops its expansion in about 43 μs, and then its velocity changes sign. Finally the velocity accelerates rapidly as the bubble collapses, reaching velocities as high as 70 m/s. We did not observe a consistent indication of bubble rebounds as reported for pulsed and acoustic cavitation. This may be attributed to the small value of the dimensionless distance that determines the dynamic behavior of the bubble [22].

Once the bubble collapses, a shockwave of very short duration is emitted. The peak amplitude of the shockwave reaches ~0.7 MPa. Figure 4 is an expanded view around the bubble collapse time as indicated by the black arrow on Fig. 3(a). The shock wave lasts only 130 ns (FWHM), however it was found that the pressure pulse emitted upon spherical bubble-cavitation collapse has a duration between 10 and 40 ns [23]. The response time of our hydrophone is 90 ns, so exposing hydrophones with comparable response time to shorter pressure pulses may underestimate the actual pressure. The hydrophone response is a combination of the impulse response and the actual signal. The FWHM of the actual cavitation pressure pulse $\tau_{cav}$ can be calculated within good approximation with the following formula [24]: $\tau_{cav}=(\tau^2_{mea} - \tau^2_{hydro})^{1/2}$ where $\tau_{mea}$ is the measured pulse width and $\tau_{hydro}$ is the FWHM response time of the hydrophone, so the actual pulse width is ~94 ns. The measured peak pressure is underestimated by a factor $m=(\tau_{cav}/\tau_{hydro})ln2$ or $m$=0.73 [23], so the actual peak pressure is 40% higher or ~1 MPa.

The peak pressure and bubble's radius averaged over 100 collapses are shown in Fig. 4(b) as function of the beam power. Note that the maximum beam power is now larger because the dichroic mirror was removed from the setup since no images were taken. It can be observed that both signals show similar dependences on power which indicates the close relationship between radius and the amplitude of the pressure wave. Both signals decay very fast, in fact for P>80 mW, the decay is exponential.

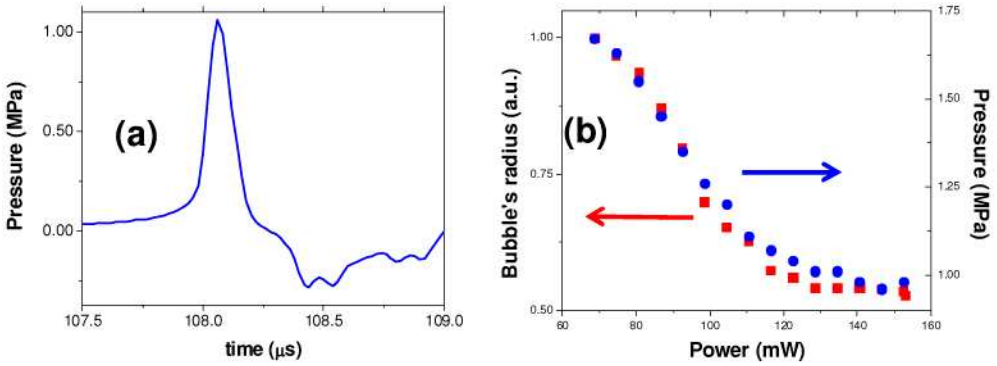


Fig. 4. (a) Typical temporal profile of the pressure pulse produced by the bubble collapse at laser power of 119 mW and (b) amplitude of the peak pressure (blue circles) and bubble radius (red squares) as function of the beam power.

All measurements of the pressure wave amplitude where performed at a fixed distance of 4 mm and we decided to study how it decays with propagation distance. Figure 5 shows that pressure wave decays as $r^{-1}$, (as indicated by the red line which is a fit to a function of the type $A/r^B$ with A and B constants) i.e. the amplitude of the pressure wave behaves as it was emitted by a spherical source. For a distance r<1 mm, the hydrophone signal randomly oscillates. The reason for such oscillations is not clear and further studies are needed in order to understand the behavior of the pressure amplitude in close proximity to the source.

#120889 - $15.00 USD Received 2 Dec 2009; revised 15 Jan 2010; accepted 24 Jan 2010; published 12 Apr 2010

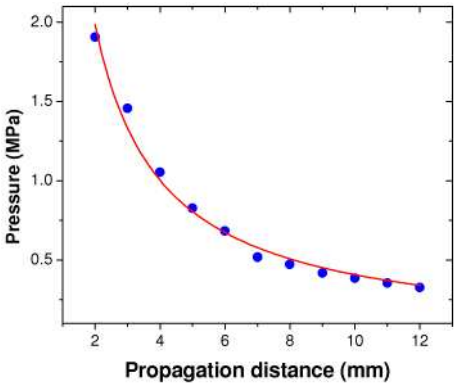


Fig. 5. Pressure wave amplitude as function of propagation distance for a power of 119 mW. The pressure decays as $r^{-1}$, as indicated by the red line.

## 4. Discussion

It is clear that by using focused low power laser in highly absorbing liquids it is possible to heat the water up to its critical limit. According to our simulations and experiments, there is a threshold intensity $I_{th}$, and therefore a threshold temperature (270 °C), for bubble formation. Once the superheat limit is reached, a violent phase explosion is observed producing an expanding vapor bubble in close proximity to the interface. The bubbles remain in contact with the substrate at all time ($\gamma$~0.5), so the bubbles possess half-hemisphere shape. Upon collapse, they behave as a point-source of pressure waves as indicated by Fig. 5. We believe this the reason why no rebound of the bubble is observed.

From our results we found that the rate of energy deposition increases with intensity i.e. the time it takes to reach its maximum temperature decreases as shown in Fig. 2. Based on this argument, under cw illumination and high intensity ($I>>I_{th}$) the bubble is created and collapses in shorter time. Thus, the cavitation frequency is higher at higher intensity; in fact, the cavitation frequency scales linearly with the intensity [17].

What it is really remarkably is that the bubble created with the lowest power produces the largest radius and therefore the highest pressure shock waves. The thermal diffusion time for water is given by $\tau_{dif}=d^2/(4D)$ where d is the distance at which the highest temperature is reached (20 μm) and D is the thermal diffusivity of water ($1.43x10^{-3}m^2/s$) [25], then $\tau_{dif}$ ~0.7 ms. For the threshold power, $\tau_{dif} << \tau_{cav}$ so heat can be transferred to a larger volume and more water is ready to be evaporated and therefore larger bubbles are produced. For $I_{max}$, $\tau_{dif}$ is comparable to $\tau_{cav}$ and therefore the vaporization volume is smaller; in consequence smaller bubbles' radius are generated. Recounting, larger vaporization volume produces larger bubbles and therefore more stored energy and released on collapse. The amplitude of the pressure wave can be enhanced by a factor of ~50 if the beam size is increased. In order to keep the intensity constant, the power must be increased in such a way to reach the superheat limit at the same rate. This fact is particularly important in laser-induced ultrasound where short pulsed lasers can be replaced with low power cw lasers. These results will be published elsewhere.

Although the streak camera provided temporal resolution of ~8 nsec, visualization of the wave front produced by the shockwave was nearly impossible due to the large jitter (few μs's) in the bubble collapse and the poor contrast of the images. The collapse time of the bubble oscillates due to stochastic nature of the nucleation probability and the random effect introduced by the light-induced water flow. However, not only the onset time of cavitation varies from pulse to pulse but also the maximum bubble radius, and therefore the pressure amplitude, varies as much as 50%. A theoretical model that explains all the observed features

#120889 - $15.00 USD Received 2 Dec 2009; revised 15 Jan 2010; accepted 24 Jan 2010; published 12 Apr 2010

is not currently available and therefore further theoretical and experimental research would be needed to attain it.

## 5. Conclusions

In conclusion, we have shown that cavitation bubbles can be produced with low CW power lasers in highly absorbing solutions. Due to the large absorption coefficient at the laser wavelength, the solution can be heated to its superheat limit (~270-300°C). Superheated water undergoes explosive phase transition around this temperature producing approximately half-hemispheric bubbles ($\gamma$~0.5). The bubbles remain in contact with the substrate at all times suppressing its rebound. On collapse, the largest pressure waves are produced by the lowest power. The bubble radius behaves in similar way to the pressure waves indicating that larger bubbles produce the highest pressure waves. The pressure waves may be capable of producing damage to the substrates, in particular, metallic and dielectric thin films. Thermocavitation can be a useful tool for the generation of ultrasonic waves and controlled ablation for use in high-resolution lithography.

## Acknowledgments

The authors acknowledge financial support from CONACyT-Mexico (Grant No. 49573-2005).

#120889 - $15.00 USD Received 2 Dec 2009; revised 15 Jan 2010; accepted 24 Jan 2010; published 12 Apr 2010